Experimental Study of Gaseous Fuel Inverse Diffusion Flame

I.A. Ibrahim [1, *], I. K. El-Kashef [2], H.M. Gad [1]

[1]Mechanical Power Engineering Department, Faculty of Engineering, Port Said University, Port Said, Egypt
[2]Mechanical Power Engineering Department, High Institute of Engineering and Technology in Arish, North Sinai, Egypt
* Corresponding author: eng.hema@eng.psu.edu.eg

A B S T R A C T

The main aim of the present work is studying the effects of swirl number and equivalence ratio on the combustion characteristics of liquefied petroleum gas (LPG) for normal diffusion flame (the NDF) and inverse diffusion flame (the IDF). The effects of different swirl numbers of 0.5, 0.75,1.0, and 1.5 are studied at an equivalence ratio of 1.0. In addition, the effect of different equivalence ratios of 0.75, 1.0, 1.5, and 2.0 at a swirl number of 0.5 were studied. The flame shape, visible flame length, temperature distributions and species concentrations were measured. To study the above parameters, a test rig that consists of an air supply line, a fuel supply line, and a burner head was designed and constructed. The results showed that, by increasing the swirl number, the visible flame length is decreased for the IDF and the NDF. Moreover, by increasing the equivalence ratio Φ, the visible flame length, for the IDF, was increased by about 39%, 91%, 108%, and 620% for air swirl number 0.5, 0.75, 1.0 and 1.5, respectively. However, the maximum temperature decreased. It was, also, found that the concentrations of NO, CO_2 and CO were increased until reach their maximum value. While the concentrations of O_2 were decreased. The maximum value of the NO for the IDF is found to be 35 ppm, while for the NDF is 245 ppm. In addition, it was found that the IDF emitted less CO and NO than the NDF did. Therefore, it is more suitable for environmental preservation.

1. Introduction

Combustion produces large amounts of energy that may be used to power automobiles, heat homes, etc. Combustion research aims to improve combustion efficiency and lower pollutant emissions [1-3]. Many combustion systems divided the fuels and oxidizers before entering the reaction zone, where mixing and combustion occur. Flame burning using gaseous fuels was studied by many researchers [4, 5]. Diffusion flame combustion systems increased the variety of operation with gaseous fuels, including extremely reactive hydrogen fuels [6]. Diffusion flames has been employed in a wide range of applications. When compared with premixed flame combustion, diffusion flame combustion has good practical value because it provides superior stability, safety, and a broad working range [7]. Inverse Diffusion Flame (the IDF) may produce both pure diffusion and premixed flames, it has the benefits of both in terms of operational safety, flame stability, and low pollutant emissions. Through increasing research focus, the IDF is projected to influence not just fuel processing but also combustion and emissions in the future [8]. Kaewpradap and Jugjai [9] examined the combustion flames using fuel and air velocity changes. Because of improved mixing between inside air and ambient air, the luminous flame length was reduced and the premixed flame length was increased by the designed the IDF burner. Lower flame length and flame temperature were obtained when the equivalence ratio was reduced. Elbaz and Robert [10] used high-speed photos of Particle Imaging Velocimetry to observe the IDF. It was indicated that increasing the air to fuel velocity ratio improves fuel entrainment into the air jet, therefore enhancing fuel-air jet mixing. Utria et al. [11] studied the multi-fuel-jet inverse diffusion flames characteristics. The results show that the oxidizer momentum influences the flame structure characteristics

These measurements indicates the flame length and the diffusion mode extension.

Patel and Shah [12] studied flame length, axial and radial temperature variations, and noise during hydrogen enrichment in swirling and non-swirling IDFs. Because of the higher fuel combustion rate and a shorter reaction zone nearby, the addition of hydrogen shorted the flame length and increased the combustion noise. In non-swirling IDFs, it has been discovered that raising the hydrogen content at constant energy addition decreased CO emissions but increased NOx emissions. Kotb and Saad [13] studied the effect of equivalence ratio on thermal efficiency for co and counter-swirl domestic burners relative to non-swirl design using LPG as a fuel. Under all operation conditions examined, the thermal efficiency of both swirl burners, i.e. co and counter burners, was larger than the non-swirled burner (base burner). The operational range of the co swirl burner was higher than that of the counter swirl burner. Kotb and Saad [14] designed co-swirl and counter-swirl burners, to investigate flame shapes, temperature distribution, and emissions under various operating conditions. The co-swirl flame with the IDF was found to be shorter and more stable than the counter-swirl flame with inverse diffusion. The flame temperature and emissions were greater in flame center for co-swirl the IDF while, counter swirl flames produced less NOx. Kotb et al. [15] studied the effects of swirling flow and porous media on the flame shape, temperature, and gas emissions of a triple coaxial ports inverse diffusion flame (TCP-IDF). The results showed that swirl reduced CO and HC emissions while increasing the peak temperature and NOx emissions. Badiger et al. [16] conducted an experimental investigation on an the IDF burner. The effect of the diameter of the air nozzle, the orientation of the fuel nozzle, and the swirl in the central air nozzle on the IDF shape were examined. Saad et al. [17] studied the effect of swirling on a double ring home LPG burner's gas hob. Four different swirl

orientation patterns were used such as: co-swirl, counter-swirl, star-pattern swirl, and radial flow. Except for the Star pattern burner, where the thermal efficiency improved but CO emissions decreased, the results showed that swirl motion enhanced both thermal efficiency and reduces CO emissions. Under all operating conditions, increasing the pan height to the burner outer diameter reduced thermal efficiency and CO emissions. Rabee et al. [18] investigated the effects of changing the diameters of the IDF burners on flame properties. The flame resembles a typical non-premixed flame with larger burner diameters, and the entrainment zone is not visible. Entrainment zone and mixing-combustion zone structure begin to appear as the nozzle size is reduced. By decreasing the nozzle diameters, the flame length was reduced, while the temperature rise rate and centerline temperatures were raised. Smaller nozzle diameters result in quicker emissions production, as well as faster depletion of the centerline oxygen concentration.

From the previous review, because of its stability and excellent emissions, the inverse diffusion flame (the IDF) is promising. The majority of the IDF publications are limited to models with short lengths. As a result, the main objective of the present work is studying the combustion characteristics of LPG inverse diffusion flame in a relatively larger test rig. The investi

gated parameters are swirl number of 0.5, 0.75, 1.5, and 2.0 and equivalence ratios of 0.75, 1.0, 1.5 and 2.0. The measured characteristics are flame shape, visible flame length, temperature patterns, and species concentrations.

2. Experimental Test Rig

To study the above parameters, an experimental test rig was designed and constructed as shown in Figure 1. The test rig consestes of several components. Firstly, a compressed air supply line which consists of a compressor, a control valve, a pressure gauge, and an air rotameter. Secondly, an LPG fuel supply line which consists of an LPG cylinder, a pressure gage, a pressure regulator valve, a fuel rotameter, and control valves to adjust the fuel path in cases of the IDF and the NDF. In the present study, the LPG fuel has a chemical composition of , by volume, 70% butane and 30% propane by volume [19]. Finally, the burner head consists of nine nozzles each with 2 mm diameter for the IDF and one central nozzle with 6 mm diameter for the NDF as shown in Figure 2. In the present study, the flame is unconfined. The burner was made up of steel with the detailed dimensions as shown in Figure 3. The burner is provided with fuel that enters in the same direction as air. The swirl number used are 0.5, 0.75, 1.0 and 1.5 with equivalence ratios of 0.75, 1.0, 1.5, and 2.0.
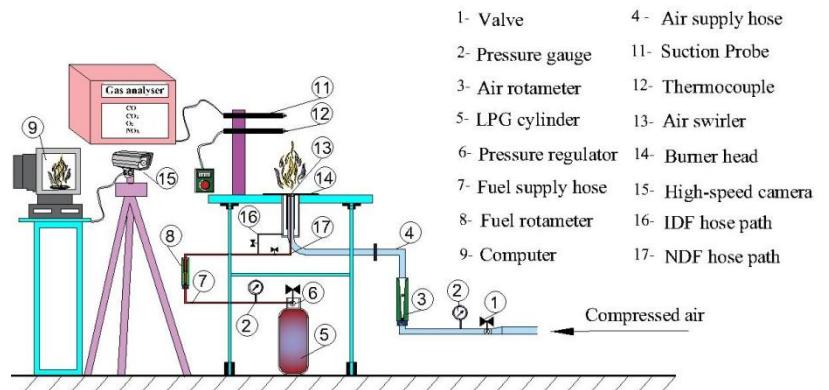

1- Valve	4 - Air supply hose
2- Pressure gauge	11- Suction Probe
3- Air rotameter	12- Thermocouple
5- LPG cylinder	13- Air swirler
6- Pressure regulator	14- Burner head
7- Fuel supply hose	15- High-speed camera
8- Fuel rotameter	16- IDF hose path
9- Computer	17- NDF hose path

Figure 1: Aphotograph and **schematic diagram of the experimental test rig**
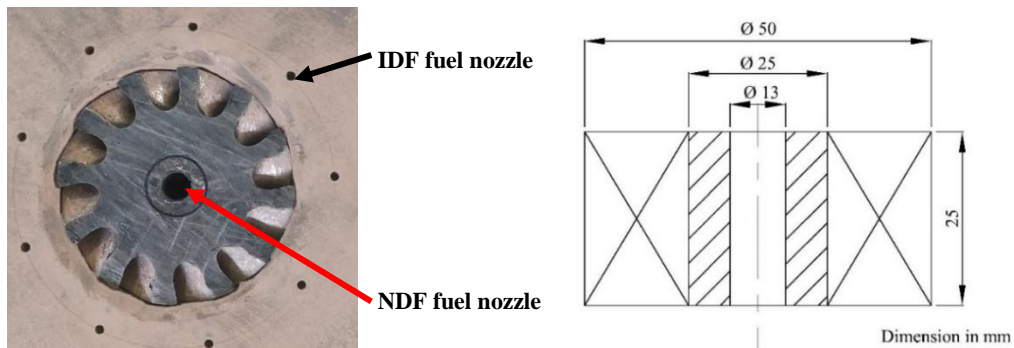

Figure 2: A photograph of the **plane view of the burner head and the detailed dimensions of the air swirler**
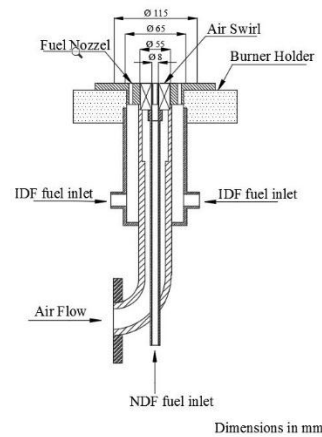
Figure 3: A photograph and detailed dimensions of the burner head

3. Experimental Results and Discussion

The experimental results consist of studying the LPG normal and inverse diffusion flame combustion characteristics such as: flame shape, visible flame length, species concentrations, and flame temperature distributions under different operating conditions including equivalence ratio of 0.75, 1, 1.5, and 2.0, and swirl number of 0.5, 0.75, 1.0 and 1.5.

3.1. Flame Shape

The flame shape in the present work is represented by flame photos taken using a digital camera, under different operating conditions. The appearance of the flame is dependent on the swirl numbers, S, and the equivalence ratios, Φ. The fuel mass flow rate was kept constant while the air mass flow rates was varied. These rates determine the overall equivalence ratio and the relationship between the impulses of the nozzles. The impulses of the nozzles help in understanding the physical processes involved in the IDF combustion. It can, also, help to differentiate between the IDF and the NDF.

The effects of changing S on the flame shape at constant Φ = 1.0 for the IDF and the NDF are shown in Figure 4. It is noticed that there is a lower blue zone surrounded by a luminous zone. By increasing the swirl number, the visible flame length is decreased for the IDF as shown in Figure 4a. For the NDF, visible flame has a small diameter as compared with the IDF, however, the NDF is longer. In addition, by increasing the swirl number, the visible flame length is decreased for the NDF as shown in Figure 4b. The flame's stability is improved significantly because of increasing S as the air has more radial momentum. This gives it more time to mix with the fuel. A good mixture will make it easier to produce a stable combustion process.

The effect of changing the equivalence ratio Φ on the flame shape at constant S = 0.5 for the IDF and the NDF are shown in Figure 5. It is shown that, by increasing the value of Φ, the flame size is increased with a slight decrease in the flame diameter for both the IDF and the NDF. A small blue region is detected in the case of the NDF at the beginning of the flame for Φ of 0.75 to 1.0, progressively decreasing until it reaches Φ = 2.0. The flame surface is wrinkled for the NDF and the flame is compact in its size for the IDF compared with the NDF. It is, also, shown that, with the increase of Φ, the air mass flow rate decreases and the flame length and size is increased for both the IDF and the NDF. In addtion, it is observed that the flame is attached for all the tested vaues of Φ.

3.2. Visible Flame Length

The visible flame length is a significant characteristic for describing the IDF and the NDF, since it aids in determining the size of the combustion chamber and provides an indicator of residence duration [20]. Figure 6 shows the effect of equivalence ratios on visible flame length for both the IDF and the NDF at different air swirl numbers. From this figure it can be seen that the flame length is increased by increasing Φ. From Figure 6a, for the IDF, it is observed that, by increasing the equivalence ratio from 0.75 to 2.0, the visible flame length is increased by about 39%, 91%, 108%, and 620% for air swirl numbers of 0.5, 0.75, 1.0 and 1.5, respectively. The maximum value of visible flame length is found at Φ = 2.0 for S = 0.5, while the minimum value is occurred at Φ = 0.75 for S = 1.5.

Figure 6b shows that, for the NDF, the visible flame length is increased by about 13%, 15%, 19%, and 18.6% for air swirl numbers of 0.5, 0.75, 1.0 and 1.5, respectively, when the equivalence ratio is increased from 0.75 to 2. Generally, when the air swirl number increases, the flame length decreases for both the the IDF and the NDF. The flame length decreases as a result of increasing chemical reaction rate, resulting in a decrease in combustion duration. Furthermore, the values of visible flame length for the NDF are very high when compared with the IDF under the same operating conditions.

3.3. Temperature Patterns

To obtain a complete characterization of temperature patterns, the temperature distributions inside the flame were measured in both the radial and the axial directions along the flame to

understand the thermal structure of the IDF and the NDF. In the present work, the temperatures of the flame were measured using a bare wire water-cooled thermocouple type B (Platinum Rhodium – 30% Platinum Rhodium – 6%). The thermocouple is introduced radially through the measuring ports arranged along with the traverse mechanism and moved with a radial increment of 10 mm as described in [21-24]. Temperature maps could be drawn under different operating conditions with the help of MS Excel for this purpose. The temperatures map is described by six temperature regions. Each region has a range of temperatures (in Kelvin) described by a certain color. The highest temperature region (from 1400 to 1600 K) is described by black color.
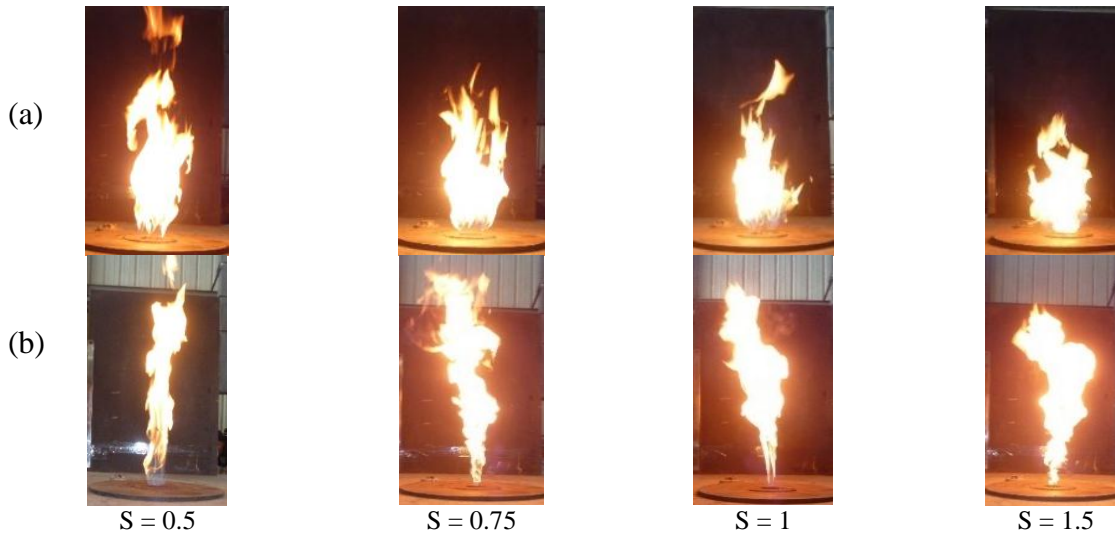

(a)

(b)

| S = 0.5 | S = 0.75 | S = 1 | S = 1.5 |

Figure 4: The effect of swirl number on flame shape for (a) the **IDF and (b)** the **NDF at Φ =1.0 and ṁ_f = 0.45 g/s**

(a)

(b)

| Φ = 0.75 | Φ = 1.0 | Φ= 1.5 | Φ = 2.0 |

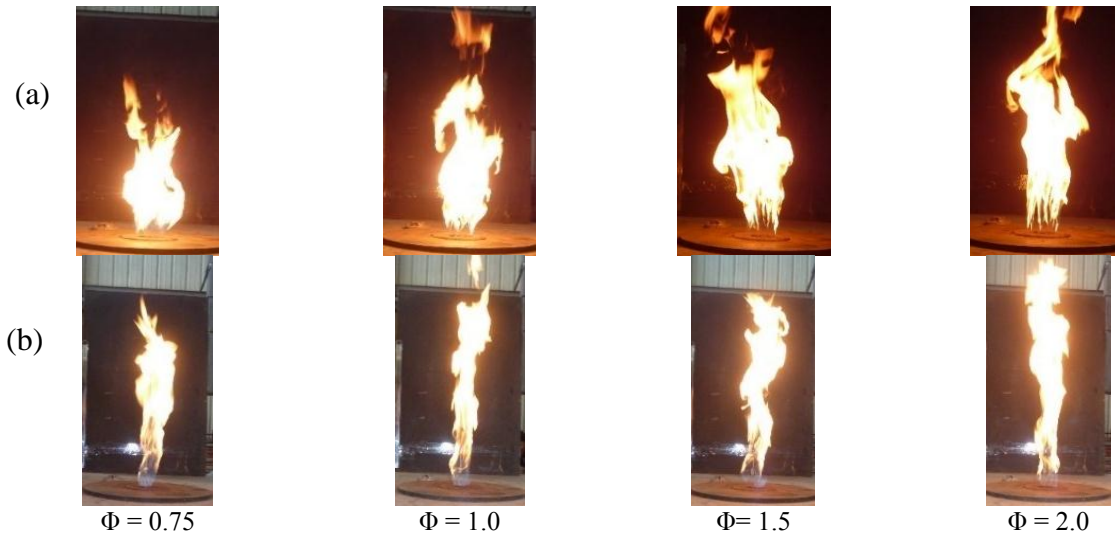**Figure 5: The effect of equivalence ratio on flame shape for (a)** the **IDF and (b)** the **NDF at S = 0.5 and ṁ_f = 0.45 g/s**
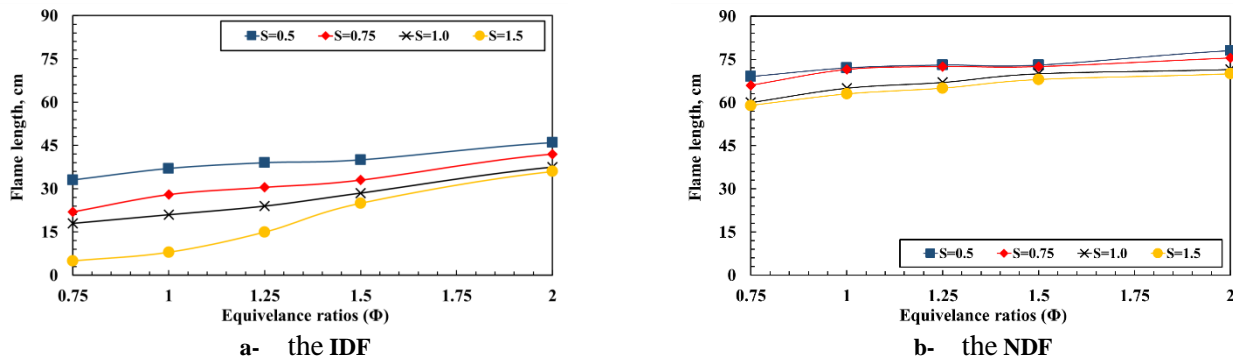

a-   the **IDF**

b-   the **NDF**

Figure 6: The effect of equivalence ratio on visible flame length for different swirl number at (a)the IDF and (b)the NDF at ṁ_f = 0.45 g/s

Figure 7 shows the effect of the equivalence ratio on the temperature maps for the IDF at S = 0.5. It is observed that the size of the high-temperature region (1400 – 1600 K) is the largest at Φ = 0.75 and is decreased with increasing the equivalence ratios until disappeared at Φ = 2.0. The region near the centerline and close to the burner head is associated with lower temperature compared with the radial region and it decreases when the equivalence ratio is increased due to the weak effect of chemical reaction in the centerline. The effect of equivalence ratio on temperature map for the NDF at S= 0.5 is shown in Figure 8. It is observed that the high temperatures region (red region from 1000 to 1200 K) is located around centerline of the flame. Moreover, by increasing the equivalence ratio, the temperature levels and flame diameter are decreased while the flame length is increased.

The effects of swirl number on temperature maps for the IDF and the NDF at Φ = 1.0 are shown in Figures 9 and 10,respectively. It is observed that the black region appears clearly with a large size at S = 1.0 and S = 1.5 for the IDF, while the highest temperature region at range of (1200-1400 K) is achieved at S = 1.0 in the case of the NDF. Figure 11 shows that the effect of equivalence ratio on maximum flame temperature for the IDF and the NDF at S = 0.5, and S = 1.0. It can be seen that, by increasing Φ from 0.75 to 2.0, the maximum temperature decreases by about 16 and 8 % for the the IDF and the NDF, respectively at S = 0.5, while the maximum temperature decreases by about 8.5 and 8 %, a for the IDF and the NDF, respectively at S= 1.0. Moreover, the maximum temperature for the the IDF is higher than that for the NDF at all air swirl numbers.
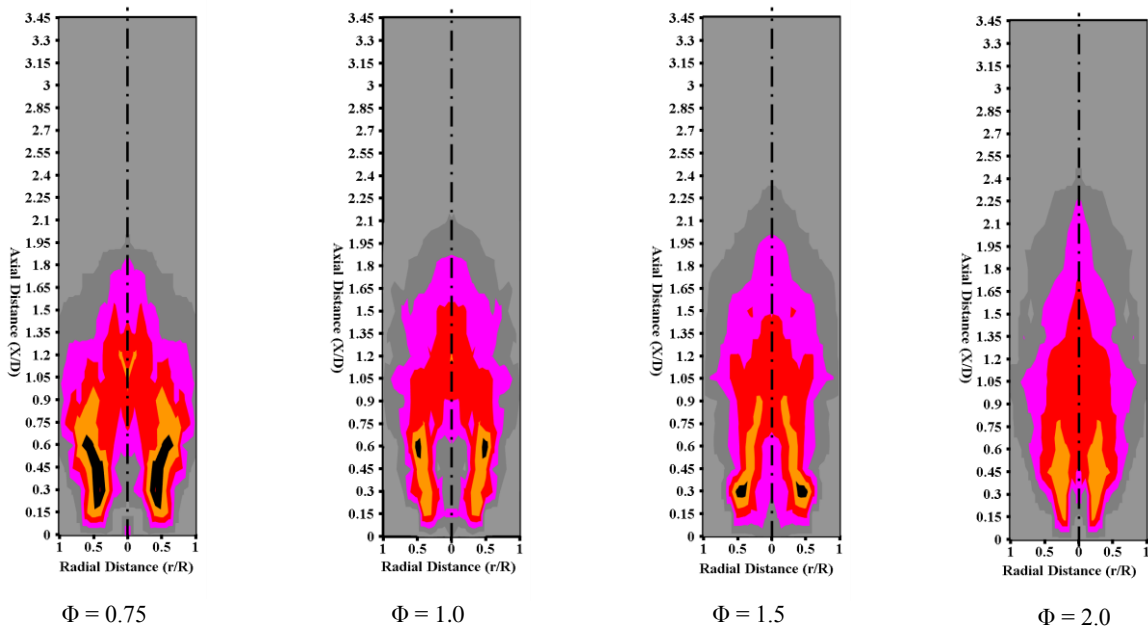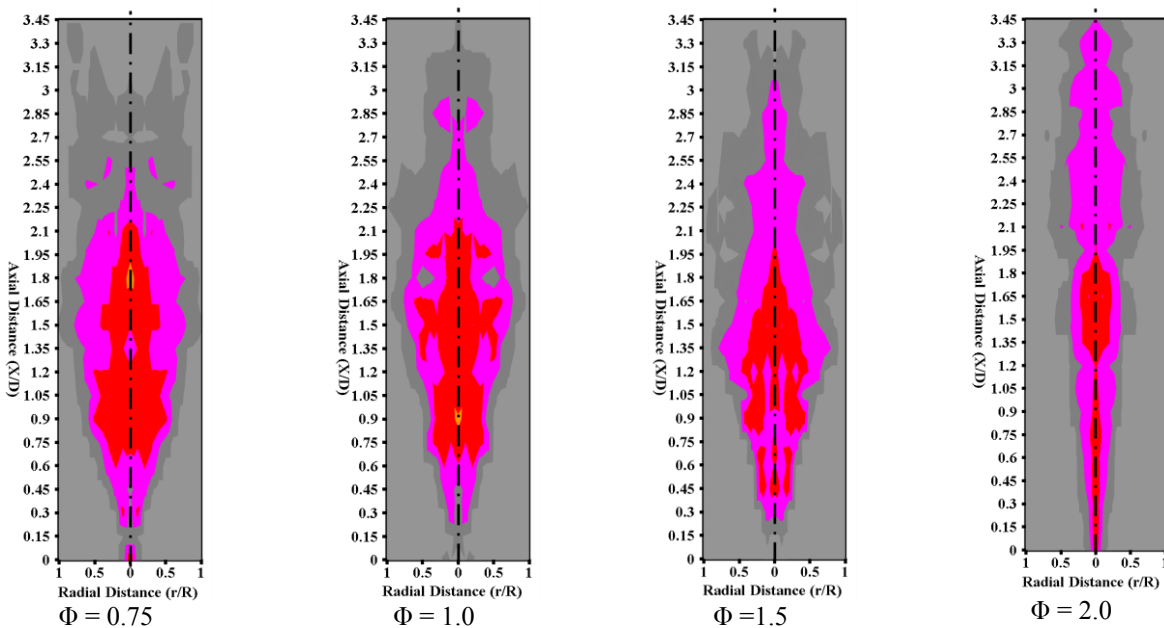

Φ = 0.75   Φ = 1.0   Φ = 1.5   Φ = 2.0

Figure 7: The effect of equivalence ratio on temperature map for IDF [S = 0.5, ṁf = 0.45 g/s]

Φ = 0.75   Φ = 1.0   Φ =1.5   Φ = 2.0

1600-1400 K   1400-1200 K   1200-1000 K   1000-800 K   800-600 K   600-400 K

Figure 8: The effect of equivalence ratio on temperature map for the NDF [S = 0.5, ṁf = 0.45 g/s]
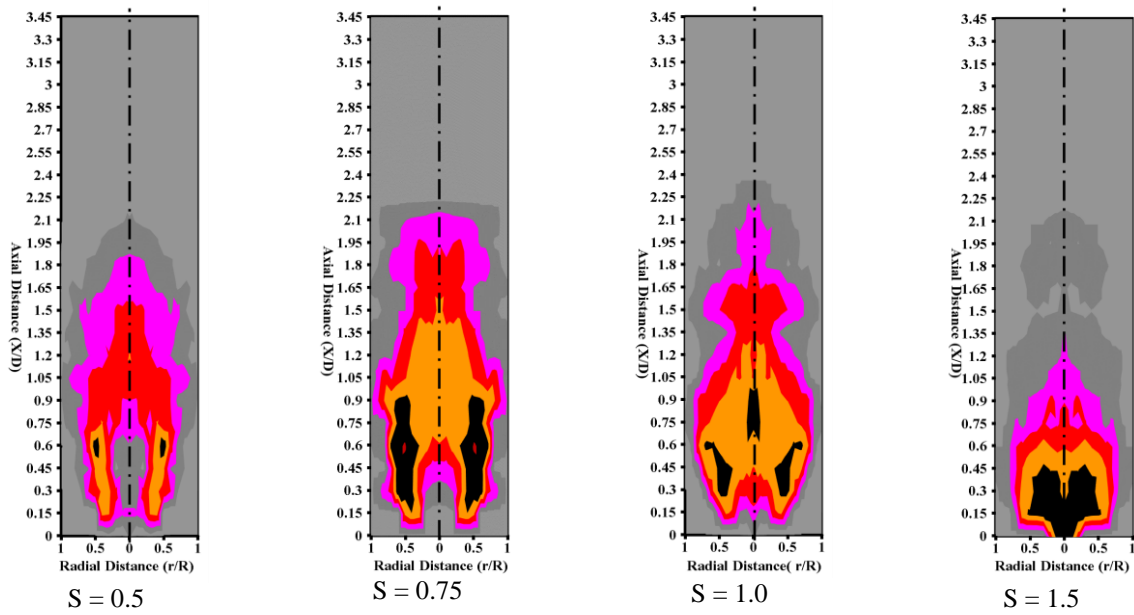

S = 0.5   S = 0.75   S = 1.0   S = 1.5

Figure 9: The effect of swirl number on temperature map for the IDF [Φ = 1.0, ṁf = 0.45 g/s]

S = 0.5   S = 0.75   S =1.0   S = 1.5

1600-1400 K   1400-1200 K   1200-1000 K   1000-800 K   800-600 K   600-400 K

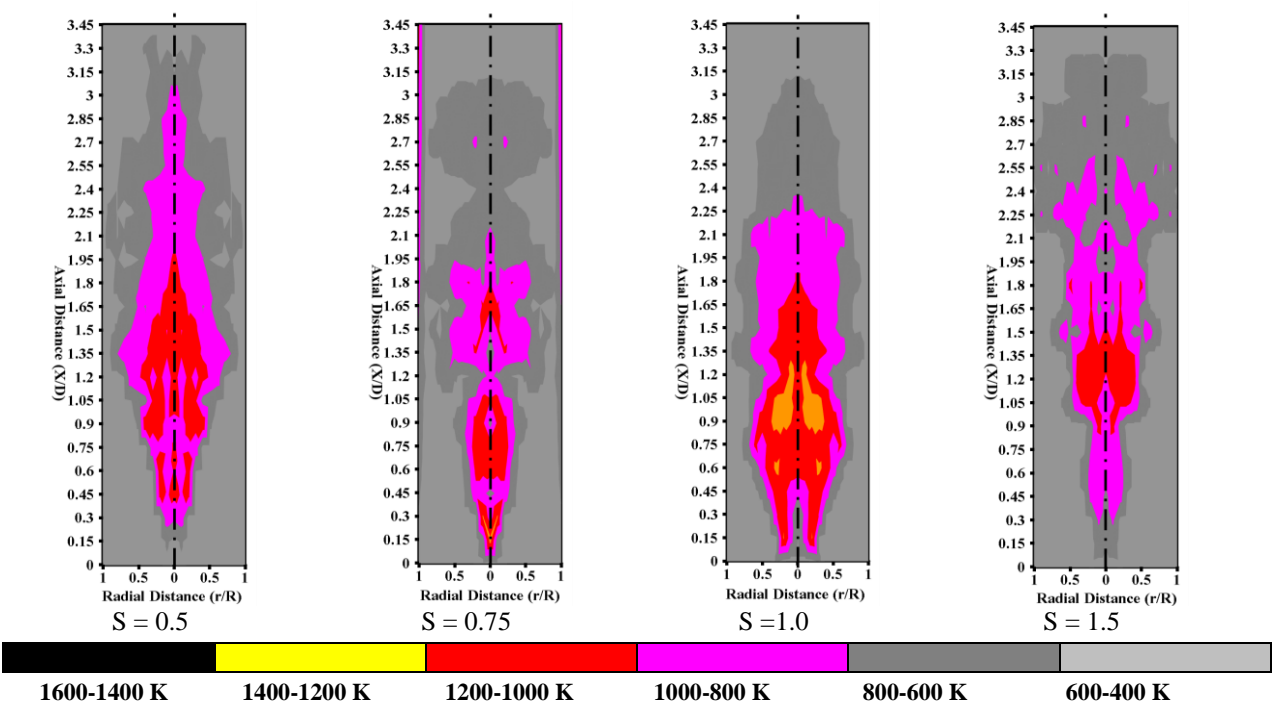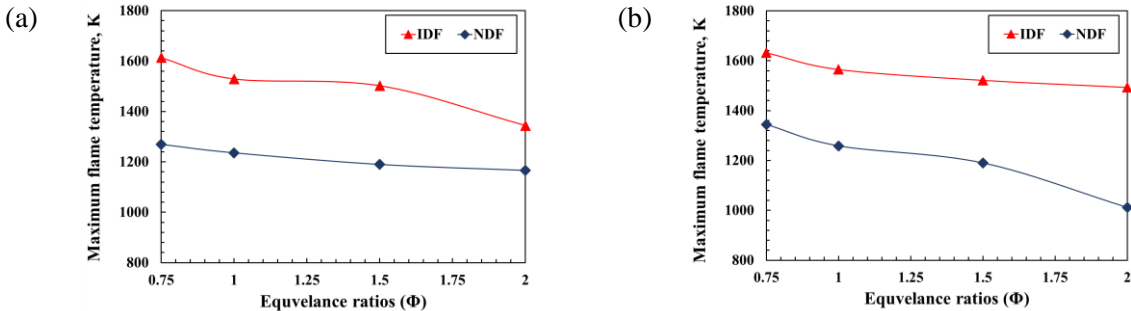**Figure 10: The effect of swirl number on temperature map for the NDF [Φ = 1.0, ṁf = 0.45 g/s]**

Figure 11: The effect of equivalence ratio on maximum flame temperature for the **NDF and** the **IDF at ṁf = 0.45 g/s for (a) S = 0.5 and (b) S = 1.0**

3.4. Species Concentrations

The composition of gas species concentrations gives information about the NO combustion process and combustion efficiency. Therefore, species NO measurements with measuring ranges of 0 -100 vol. %, 0 - 5 vol. % and 0 - 5000 ppm, respectively and Magnos 206 for O_2 measurement with a measuring range of 0 – 21 vol. %). The species concentrations were measured and presented at the axial centerline for S = 0.5. The species concentrations for different equivalence ratios for the IDF at S = 0.5 are shown in Figure 12. It is observed that, by moving axially downstream inside the flame center, the concentrations of NO, CO_2 and CO are increased until reaching their maximum values at X/D = 0.6 to 1.08 while the concentrations of O_2 are decreased.

Figure 13 shows the effect of variation of Φ on the concentrations of NO with temperature, for the IDF. It is observed that, by increasing the equivalence ratio, NO concentrations are steadily raised until they reach their maximum at the peak temperature value and become closer to the beginning of burner. It is found that, for Φ = 0.75, the peak value of NO and temperature is occurred at X/D = 1.08, while it occurred at X/D = 0.75 at Φ = 2.0. In the case of the NDF, the concentrations of NO, CO_2 and CO have the maximum values at the beginning of the burner as shown in Figure 14. This indicate that the chemical reaction is started after burner head directly. It is observed that the maximum value of NO for the IDF is found to be 35 ppm, while for the NDF it is 245 ppm. In general, NO concentrations vary with the temperature of the primary reaction zone. Because the flame is largely premixed in nature, the temperature of the flame rises because of two factors can impact the mean flame temperature and the residence time of the flame gases in the high-temperature flame zone as a result of the internal recirculation zone.

In the IDF, the CO concentration is observed to be lower than that in the NDF. The emission of CO at low Φ is attributed to the extended effect of the flame cooling, further reducing the temperature of the flame. Thereafter, the concentration decreases due to dilution of the flue gas by the entrained ambient air and due to oxidation of CO to CO_2. It is observed that the CO concentration reaches the peak value of 2900 ppm for the IDF at Φ = 1.5 and 35000 ppm for the NDF at Φ = 1.0. The percentage of the O_2 concentration decreases when the concentration of the rest of the previous emissions increases, which indicates that the oxygen has been consumed during the chemical reaction process.

Figure 15 shows the axial centerline NO concentrations and gas temperature profiles for different Φ in the case of the NDF with S = 0.5. It can be seen that both NO and gas temperature curves have the same trend, and the maximum values of the NO concentrations occur at the same position where the maximum temperature takes place. This indicates that the thermal NO mechanism is the predominant one according to Zeldovich mechanism that describes the oxidation of nitrogen and NOx formation [23].
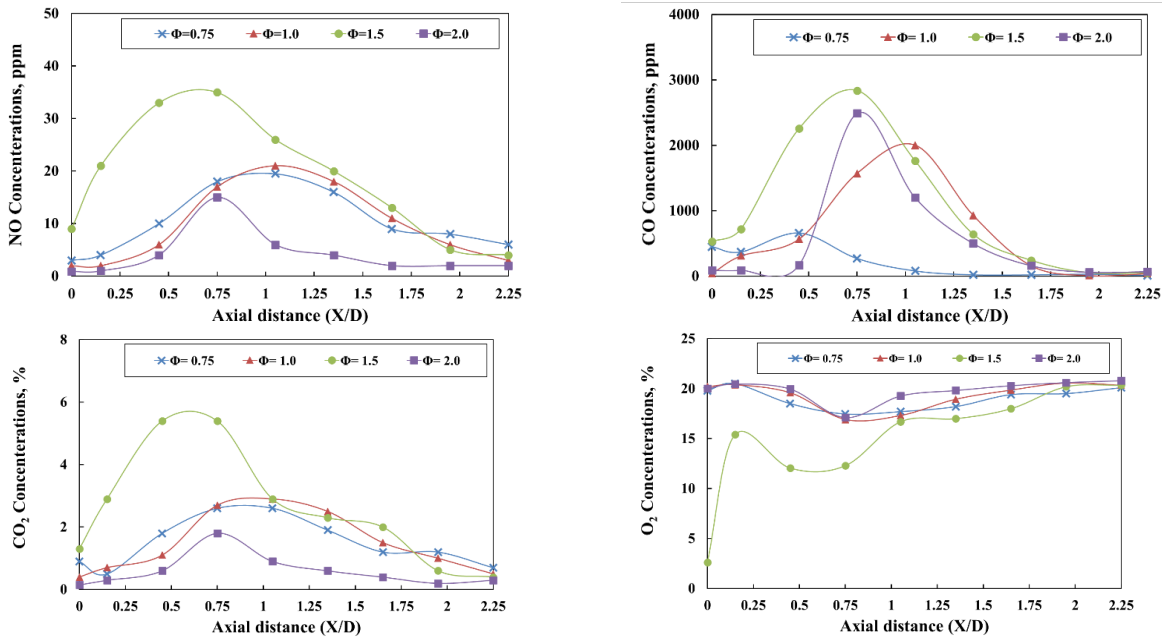

Figure 12: Axial center line species concentrations for different Φ at the **IDF, S = 0.5**
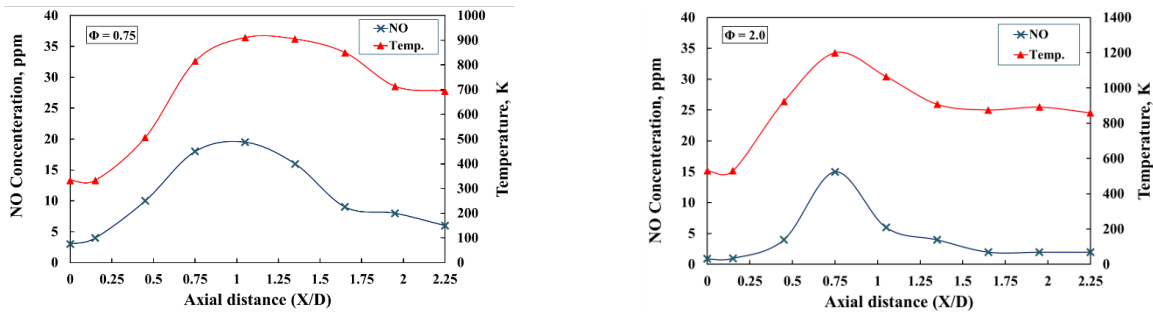
Figure 13: Axial center line NO concentrations with temperature at different Φ for the IDF, S = 0.5
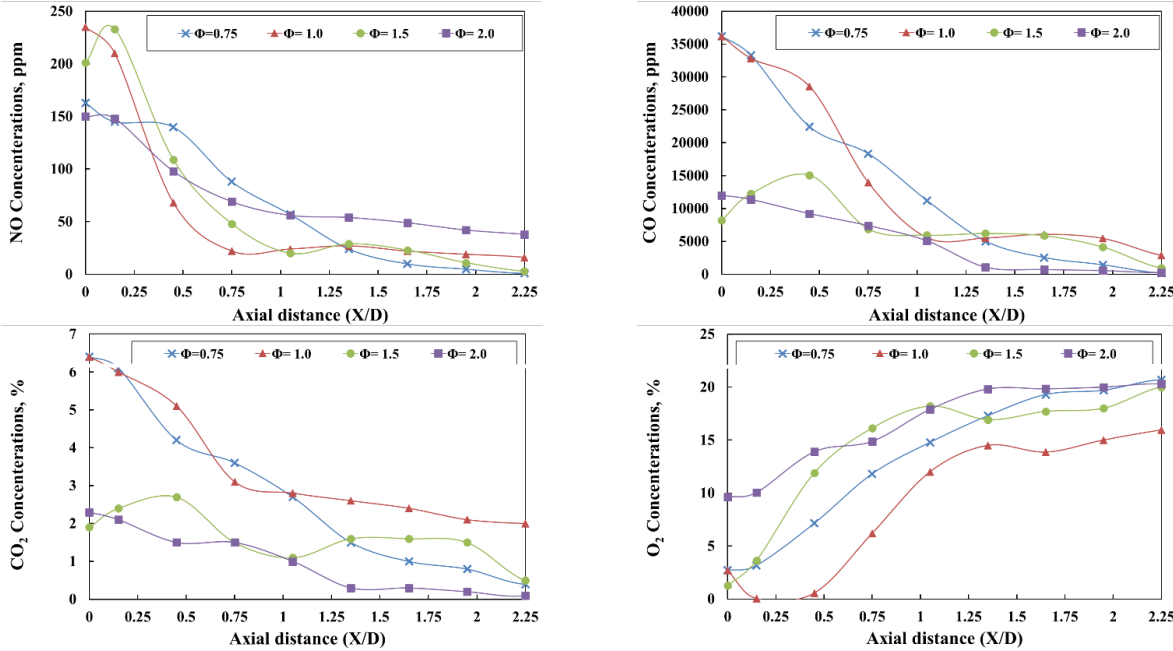

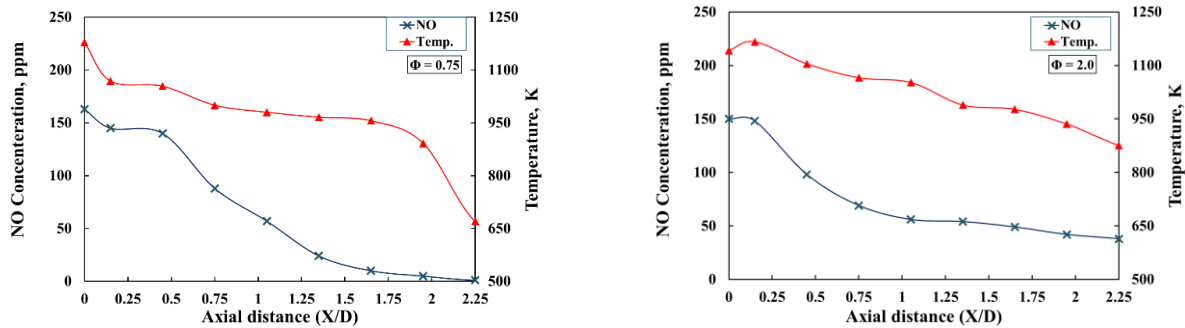**Figure 14: Axial center line species concentrations for different Φ at the NDF, S = 0.5**

Figure 15: Axial center line NO concentrations with temperature for different Φ at the NDF, S = 0.5

4. Conclusion

From the experimental results of the present study and by changing the combustion air swirl number as 0.5, 0.75, 1.0, and 1.5, and equivalence ratio as 0.75, 1.0, 1.5, and 2.0, and measuring the flame shape, visible flame length, temperature patterns, and species concentrations are measured, the following conclusions can be drawn:

- By increasing Φ from 0.75 to 2.0, the flame size increased with a slight decrease in flame diameter for the IDF.

- By increasing Φ from 0.75 to 2.0, the visible flame length, for the IDF, increased by about 39%, 91%, 108%, and 620% for air swirl number 0.5, 0.75, 1.0 and 1.5, respectively.

- The maximum value of the visible flame length, for the IDF, was found at Φ = 2.0 for S = 0.5, while the minimum value was occurred at Φ = 0.75 for S = 1.5.

- By increasing Φ from 0.75 to 2.0, the maximum temperature decreased by about 16 and 8 % for the IDF and the NDF, respectively at S = 0.5, while the maximum temperature decreases by about 8.5 and 8 %, a for the IDF and the NDF, at S= 1.0.

- The species concentrations of NO, CO_2 and CO were increased until reaching their maximum values then decreased, while, the concentrations of O_2 were decreased.
- By increasing S, the visible flame length decreased for the IDF and the NDF.
- By increasing S, the values of the IDF visible flame length were very large compared with IDF at the same operating condition.
- The peak concentration value of NO is close to the high-temperature zone then the concentration of NO is decreased gradually towards the end of the flame.

Conflict of Interest

The authors declare no conflict of interest.

References

[1] McManus N. N., Ignitable and Explosive Atmospheric Hazards, in Safety and Health in Confined Spaces, 2018.

[2] Huang Y., Li B., Liu D., Xie X., Zhang H., Sun H. and Zhang S, "Fundamental advances in biomass autothermal/oxidative pyrolysis", ACS Sustainable Chemistry & Engineering, vol.**8**, No. **(32)**, 11888-11905, 2020. https://doi.org/10.1021/acssuschemeng.0c04196.

[3] Zhou L., Song Y., Ji W. and Wei H. (2022), "Machine learning for combustion", Energy and AI, vol. **7**, 2022. https://doi.org/10.1016/j.egyai.2021.100128.

[4] Karyeyen S., Feser J.S. and Gupta A.K., "Swirl assisted distributed combustion behavior using hydrogen-rich gaseous fuels", Applied Energy, vol. 251, 113354, 2019. https://doi.org/10.1016/j.apenergy.2019.113354.

[5] Sun X., Liu H., Duan X., Guo H., L Y., Qiao, J. and Liu J., "Effect of hydrogen enrichment on the flame propagation, emissions formation and energy balance of the natural gas spark ignition engine", Fuel, vol. **307**, 121843, 2022. https://doi.org/10.1016/j.fuel.2021.121843.

[6] Brun K., Allison T. C. and Dennis R., "Thermal, Mechanical, and Hybrid Chemical Energy Storage Systems", Academic Press, 2020.

[7] Abdelaal M. M., Ali S. M., Radwan A. M. and Ismail A. A., "Investigation of a new design of inverse diffusion flame burner", Journal of Al-Azhar University Engineering Sector, 11(41), 1299-1309, 2016. https://doi.org/10.21608/auej.2016.19349.

[8] Zhen H. S., Wei Z. L., Liu X. Y., Liu Z. H., Wang X. C., Huang Z. H. and Leung C. W., "A state-of-the-art review of lab-scale inverse diffusion burners & flames: From laminar to turbulent", Fuel Processing Technology, 222, 106940, 2021. https://doi.org/10.1016/j.fuproc.2021.106940.

[9] Kaewpradap A. and Jugjai S., "Improvement of IDF Burner Effects on Lean Non-Premixed Synthetic Thai Natural Gas Flames", IOP Conference Series: Earth and Environmental Science, vol. **265**, 012002, 2019. doi.org/10.1088/1755-1315/265/1/012002.

[10] Elbaz A. M. and Roberts W. L. "Flame structure of methane inverse diffusion flame", Experimental thermal and fluid science, vol. **56**, 23-32, 2014. https://doi.org/10.1016/j.expthermflusci.2013.11.011,

[11] Utria K., Labor S., Kühni M., Escudié D. and Galizzi C., "Experimental study of H2/O_2 downward multi-fuel-jet inverse diffusion flames", Experimental Thermal and Fluid Science, vol. **134**, 110583, 2022. https://doi.org/10.1016/j.expthermflusci.2021.110583.

[12] Patel V. and Shah R. "Effect of hydrogen enrichment on combustion characteristics of methane swirling and non-swirling inverse diffusion flame", International Journal of Hydrogen Energy, vol. **44**, No. (52), 28316-28329, 2019. https://doi.org/10.1016/j.ijhydene.2019.09.076.

[13] Kotb A. and Saad H., "Case study for co and counter swirling domestic burners", Case studies in thermal engineering, vol. **11**, 98-104, 2018. https://doi.org/10.1016/j.csite.2018.01.004.

[14] Kotb A. and Saad H., "A comparison of the thermal and emission characteristics of co and counter swirl inverse diffusion flames", International Journal of Thermal Sciences, vol. **109**, 362-373, 2016. https://doi.org/10.1016/j.ijthermalsci.2016.06.015.

[15] Kotb A., Kamal M. M., Baghdady A. and Saad H., "Case study for swirling flow and porous media on triple coaxial ports inverse diffusion flame", Alexandria Engineering Journal, vol. **61** No. **(3)**, 2294-2306, 2022. https://doi.org/10.1016/j.aej.2021.07.017.

[16] Badiger S., Anil T. R., Hindasageri V. and Katti V. V., "Heat transfer characteristics of an inverse diffusion flame with induced swirl", Journal of the Brazilian Society of Mechanical Sciences and Engineering, vol. **42, No.** (5), 1-14, 2020. https://doi.org/10.1007/s40430-020-02330-5.

[17] Saad H. E., Kamal M. and Adel A., "Thermal and combustion characteristics of a double ring burner with different swirling flow patterns", In International Conference on Aerospace Sciences and Aviation Technology, vol. **18**, No. **(18)**, 1-13, 2019. https://doi.org/10.1088/1757-899X/610/1/012042.

[18] Rabee B. A., "The effect of inverse diffusion flame burner-diameter on flame characteristics and emissions", Energy, vol. **160**, 1201-1207, 2018. https://doi.org/10.1016/j.energy.2018.07.061.

[19] Sze L. K., Cheung C. S. and Leung C. W. "Appearance, temperature, and NOx emission of two inverse diffusion flames with different port design", Combustion and flame, vol. **144**, No. **(1-2)**, 237-248, 2006. https://doi.org/10.1016/j.combustflame.2005.07.008.

[20] Salman A. M., Ibrahim I. A., Gad H. M. and Farag T. M., "Effects of air temperature on combustion characteristics of LPG diffusion flame", Materials science, vol. **1008**, 128-138, 2020.https://doi.org/10.4028/www.scientific.net/MSF.1008.128.

[21] Amer, A. A., Gad, H. M., Ibrahem, I. A., Abdel-Mageed S. I., and Farag, T. M., "Experimental Study of LPG Diffusion Flame at Elevated Preheated Air Temperatures", World Academy of Science, Engineering and Technology, International Journal of Mechanical, Aerospace, Industrial, Mechatronic and Manufacturing Engineering Vol. **9**, No. **(8)**, 2015. https://doi.org/10.5281/zenodo.1108072.

[22] Gad H. M., Farag T. M. and Ibrahim I. A., "Effect of fuel nozzle geometry on LPG diffusion flame" International Journal of Advanced Scientific and Technical Research, vol. **7**, 498-511, 2015.

[23] Ibrahim I. A., Shokry A.H., Shabaan M.M., Gad H.M., " A comparative study of gaseous fuel flame characteristics for different bluff body geometries", Case Studies in Thermal Engineering, vol. **34**, 101951, 2022. https://doi.org/10.1016/j.csite.2022.101951.

[24] Ahmed R., Galal A.I.A, EL-Sharkawy M.R., " Waste heat recovery for hybrid electric vehicles using thermoelectric generation system", Journal of Advanced Engineering Trends (JAET), vol. **38**, No. **(2)**, 173-184, 2019. https://doi: 10.21608/JAET.2020.73077

Abbreviation and symbols

D	Burner diameter, 20 cm
IDF	Inverse diffusion flame
L_f	Flame length, cm
LPG	Liquefied Petroleum Gas
NDF	Normal diffusion flame
R	Burner radius, 10 cm
r/R	Dimensionless radial distance
S	Swirl number
X/D	Dimensionless axial distance
Φ	Equivalence ratio